



# Magnetic resonance imaging findings of central nervous system in lysosomal storage diseases: A pictorial review

Nathan Fagan,<sup>1</sup> Allen Alexander,<sup>1</sup> Neville Irani,<sup>2</sup> Charbel Saade<sup>3</sup> and Lena Naffaa<sup>3</sup>

<sup>1</sup> Department of Diagnostic Radiology, Aultman Hospital, Canton, Ohio, USA

<sup>2</sup> Department of Diagnostic Radiology, University of Kansas, Medical Center, Kansas City, Kansas, USA

<sup>3</sup> Department of Diagnostic Radiology, American University of Beirut, Medical Center, Beirut, Lebanon

**N Fagan MD; A Alexander MD; N Irani MD;  
C Saade PhD; L Naffaa MD.**

## Correspondence

Dr Lena Naffaa, Department of Diagnostic Radiology, American University of Beirut, Medical Center, PO Box: 11-0236, Riad El Solh, Beirut 11072020, Lebanon.  
E-mail: ln01@aub.edu.lb

Conflict of interest: None.

Submitted 10 June 2016; accepted 5 November 2016.

doi:10.1111/1754-9485.12569

## Introduction/Background

Lysosomal storage diseases (LSD) are a group of rare inherited metabolic disorders that are a result of inborn errors of metabolism. They are a clinically heterogeneous group of approximately 50 disorders that are classified according to the accumulation of an improperly degraded macromolecule in tissues.<sup>1</sup>

The lysosome is a cellular organelle with the purpose of digesting larger macromolecules. It accomplishes this task through the use of catabolic enzymes and an acid-rich environment. The list of macromolecules that are degraded through the lysosome include sphingolipids, glycoproteins and glycosaminoglycans. LSDs result when there is a disruption in the pathway of elimination for such molecules. The particular symptoms of the disease are primarily dependent on the substrate tissue source and the relevant metabolic pathway that is disrupted leading to a build-up of the substrate in the tissues. The most common defects involve lipids and are closely related.<sup>1</sup>

More than 40 of the classified LSDs share some level of decreased T2 signal by magnetic resonance imaging (MRI) or increased attenuation by computed tomography (CT) in the bilateral thalami. This is felt to be due to excess deposition of the undigested metabolites which

## Summary

Lysosomal storage diseases (LSD) are a complex group of genetic disorders that are a result of inborn errors of metabolism. These errors result in a variety of metabolic dysfunction and build-up certain molecules within the tissues of the central nervous system (CNS). Although, they have discrete enzymatic deficiencies, symptomatology and CNS imaging findings can overlap with each other, which can become challenging to radiologists. The purpose of this paper is to review the most common CNS imaging findings in LSD in order to familiarize the radiologist with their imaging findings and help narrow down the differential diagnosis.

**Key words:** central nervous system; imaging findings; lysosomal storage diseases; magnetic resonance imaging.

results in an increased viscosity leading to T1 and T2 shortening.<sup>2</sup> The classic LSD finding is tigroid white matter, which is thought to be related to periventricular lipid accumulation on a background of absent myelin<sup>2</sup> (Fig. 1). Additional neuroimaging findings demonstrate significant overlap between syndromes. The purpose of this paper is to review the most common LSDs, familiarize the radiologist with their imaging findings in order to aid in narrowing the differential diagnosis. The most common disorders will be discussed in this article and include: Metachromatic leukodystrophy (MLD), Krabbe's disease, the gangliosidoses Fabry's disease, neuronal ceroid lipofuscinosis and the mucopolysaccharidoses.

## Metachromatic leukodystrophy

Metachromatic leukodystrophy is the result of deficiency in arylsulfatase A (ARSA) or, even rare, of its activator protein sapropterin-4.<sup>3</sup> All cases result in the accumulation of the ARSA substrate galactosylceramide I<sup>3</sup>-sulfate in the white matter of the central and peripheral nervous system.<sup>3</sup> Sulfatides are a component of myelin and it has been postulated that their build-up in patients with MLD may eventually lead to myelin breakdown.<sup>4</sup> It is an autosomal recessive disorder resulting from a mutation in the ARSA gene located on chromosome 22q13.31.<sup>5</sup> The

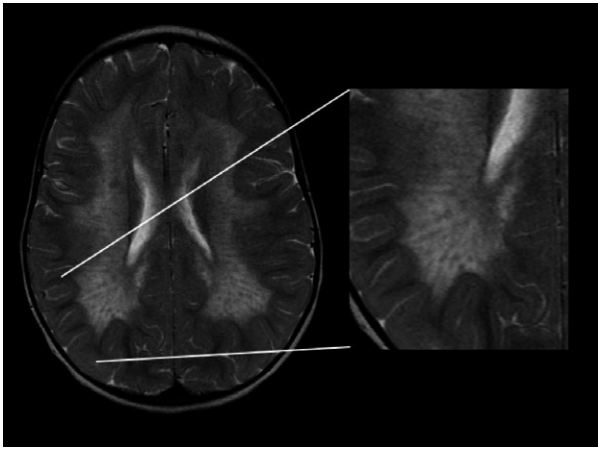


**Fig. 1.** Axial T2-weighted image through the brain showing the classic finding among the majority of LSD cases, 'tigroid' appearance to the periventricular white matter. Findings are thought to be related to periventricular lipid accumulation (low signal) on a background of absent myelin (high signal).

disease is classified according to the age at onset into the following: Infantile (1–4 years), juvenile (5–10 years) and adult (after puberty). Infantile is the most common form accounting for 60–70% of all cases.<sup>1</sup> Clinical manifestations are dependent on the age of onset. Infantile MLD will usually present with painful polyneuropathy and progressive gait disturbances between the ages of 14–16 months.<sup>1</sup> Gait disturbances are progressive with affected patients eventually being unable to sit up or stand.<sup>1</sup> The juvenile and adult forms have a similar presentation with behavioural abnormalities, cognitive deficits and dementia as more prominent features.<sup>6</sup> Age of onset is typically 5–10 years in the juvenile form with adult being classified as anything after the onset of puberty.<sup>7</sup> Common features of all forms include gallbladder dysfunction and early megalencephaly. Gallbladder dysfunction is the result of deposition of sulfatides in the gallbladder resulting in sludge or polypoid ingrowths which may result in acute cholecystitis.<sup>8</sup>

The neuroimaging hallmark of MLD is a rapidly progressive leukodystrophy with periventricular white matter predominance. The typical MRI appearance is symmetric, confluent, 'butterfly' T2/FLAIR hyperintensity in bilateral periventricular white matter.<sup>9</sup> There is early sparing with later involvement of the subcortical U-fibres, internal capsule and corpus callosum. Low T2/FLAIR signal may be seen in the thalami, however, less so than Krabbe's disease.<sup>9</sup> A tigroid appearance to the white matter on T2-weighted imaging may be evident secondary to islands of normal myelin around medullary veins producing linear hypointensities in confluent hyperintensity<sup>9</sup> (Fig. 2). Diffusion weighted imaging (DWI) often demonstrates restricted diffusion in the involved white matter<sup>9</sup> (Fig. 3). Enhancement of the cranial nerves may also be seen<sup>9</sup> (Fig. 4). Short TE (35) MR

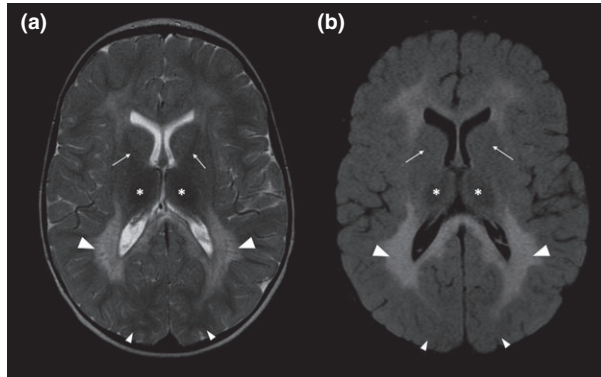


**Fig. 2.** Axial T2 (a) and FLAIR (b) images in a patient with MLD. The images depict some of the typical findings in MLD. The hallmark of the disorder is rapidly progressive leukodystrophy with the periventricular white matter taking on the typical MRI appearance of symmetric, confluent, 'butterfly' T2/FLAIR hyperintensity, often with a tigroid appearance (large arrowheads). There is usually early sparing with later involvement of the subcortical u-fibers (small arrowheads) and internal capsule (small arrows). Low signal is seen within the bilateral thalami, a feature in many LSDs (asterix).

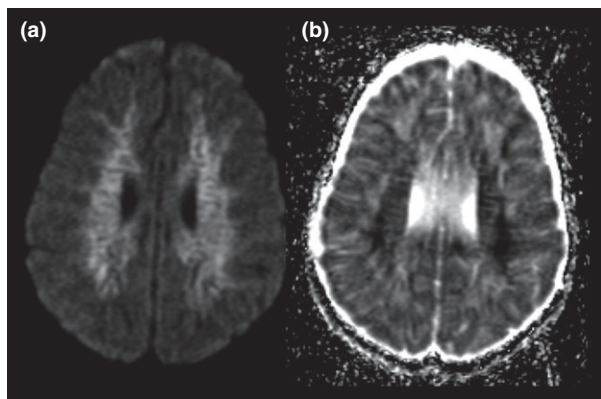


**Fig. 3.** Diffusion-weighted imaging in patients with MLD will often show diffusion restriction in the affected white matter. In the above example, we can see diffuse involvement of the white matter evident by restricted diffusion on both the DWI image (a) and the ADC map (b).

spectroscopy in the abnormal periventricular white matter may demonstrate relative elevation in the choline band with variable elevation of myoinositol<sup>9</sup> (Fig. 5).

No effective treatment exists for the disease. However, when undertaken early, bone marrow transplantation may slow or halt the progression of the disease<sup>1</sup> (Fig. 6). Unfortunately bone marrow transplantation may fail, particularly when neuropsychologic signs are advanced<sup>1</sup> (Fig. 7).

### Krabbe disease

Krabbe's disease (or Globoid Cell Leukodystrophy, GLD) is a disease that is a result of a galactocerebroside

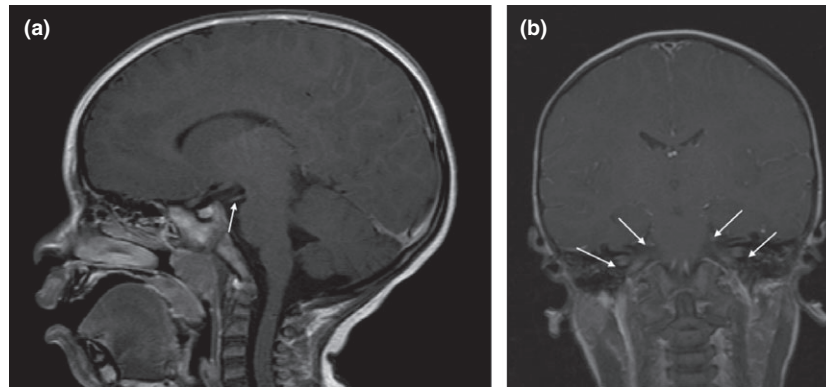


**Fig. 4.** Enhancement of the cranial nerves (CNs) is a common finding in multiple LSDs. The above post-contrast enhanced sagittal and coronal T1-weighted images demonstrate enhancement of CNs III (a, arrow) as well as CNs V, VII, and VIII (b, arrows).

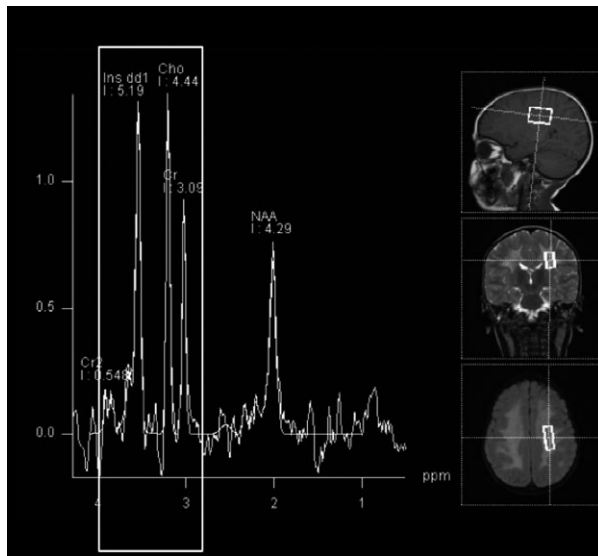


**Fig. 5.** Short TE (35) single voxel MR spectroscopy in a patient with MLD. Abnormal periventricular white matter in patients with MLD demonstrates decreased NAA peak with relative elevation in the choline band with variable degrees of elevation in myoinositol on MR spectroscopy. The above case depicts a case in which both the choline and myoinositol bands are elevated.

betagalactosidase deficiency<sup>10</sup>. The normal function of galactocerebroside betagalactosidase is to cleave the bond between ceramid and galactose in the molecule of galactosylceramide. The end result is an accumulation of galactosylsphingosine in oligodendrocytes and macrophages.<sup>11</sup> Galactosylsphingosine is highly toxic to oligodendrocytes leading to severe myelin loss from oligodendrocyte destruction.<sup>11</sup> GLD is an autosomal recessive disorder caused by mutations in the galactosylceramidase gene located on chromosome 14q31.<sup>11–13</sup> Infantile, juvenile and adult forms are recognized. The majority of cases are an early infantile form (onset between 1–6 months old) with the later onset forms

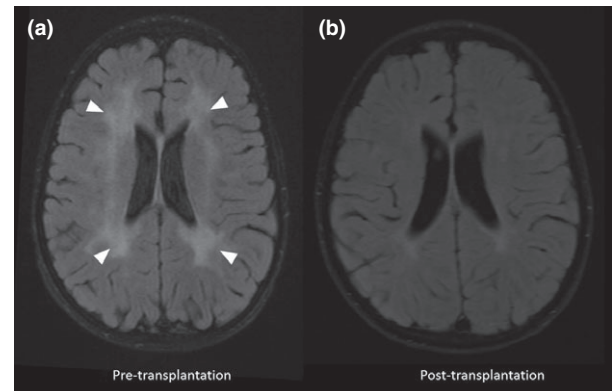


**Fig. 6.** Axial FLAIR images (a) pre and (b) post bone marrow transplant. (a) Pre-bone marrow transplantation axial FLAIR image in a 15-month-old infant boy with MLD shows symmetric 'butterfly' hyperintensity of the periventricular white matter (arrowheads). BMT was performed at the age of 4 years with significant improvement in the abnormal 'butterfly' hyperintensity of the periventricular white matter as seen in axial FLAIR image (b) obtained at the age of 5 years.

being exceedingly rare.<sup>12</sup> Patients demonstrate rapid psychomotor regression with generalized rigidity with tonic spasms.<sup>12</sup> Opisthotonic posturing is common with clenched fists and myoclonic jerks.<sup>12</sup> Blindness and optic atrophy are features that appear later in the disease process.<sup>12</sup>

The MR imaging in patients with infantile GLD shows demyelination and gliosis without inflammation (non-enhancing) in the cerebrum and cerebellum.<sup>12</sup> The corpus callosum is often involved earlier in the disease process with the subcortical U-fibers spared until late in the disease<sup>12</sup> (Fig. 8). GLD is one of the few leukodystrophies in which cerebellar findings may appear earlier in the disease. Similar to MLD, T2 hypointense, tigroid stripes in the periventricular white matter can be seen in a background of hyperintense signal<sup>12</sup> (Fig. 8). Also similar to MLD, cranial nerve enhancement and a low T2 signal in the bilateral thalami may be seen. However, GLD will often

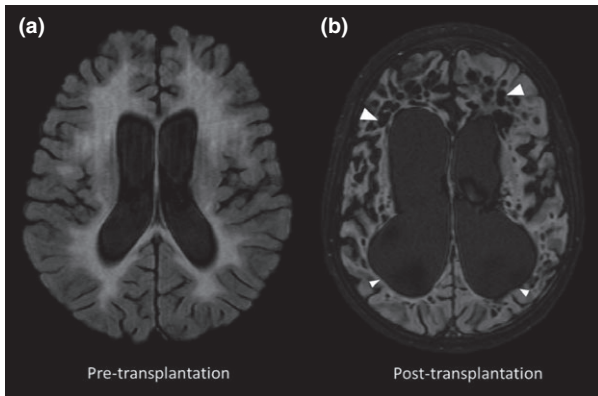


**Fig. 7.** (a) Pre- and (b) post-bone marrow transplant FLAIR imaging in a patient with MLD shows interval progression of disease. Specifically, there is severe volume loss and dilation of the ventricles (small arrowheads) secondary to periventricular white matter necrosis and resultant cyst formation (large arrowheads). All findings point to worsening leukomalacia.

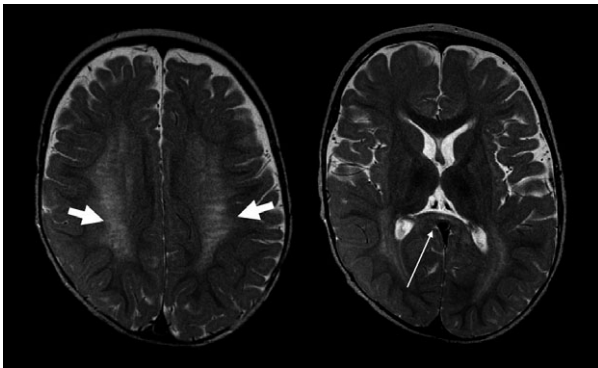


**Fig. 8.** Axial T2-weighted images in a 6-year-old male with Krabbe's disease. The above axial T2-weighted images show findings commonly seen in patients with Krabbe's disease. Often, like many other LSDs, the periventricular white matter will take on a tigroid appearance (large arrows). However, unlike the others, the corpus callosum is often involved earlier in the disease process (small arrow).

demonstrate preferential involvement of optic nerves and a greater decrease in the T2 signal from the thalami compared to MLD<sup>12</sup> (Fig. 9). Additionally, increased attenuation is seen within the thalami on non-contrast enhanced CT (NECT) early in the course<sup>12</sup> (Fig. 10). Although the true cause is unknown, it has been postulated to be secondary to alterations in the ratio of lipids, water, and proteins in response to the disease. Late stages of the disease show generalized atrophy.<sup>12</sup>

### Fabry disease

Fabry disease (FD) is the result of an alpha galactosidase-A deficiency. This leads to a progressive accumulation of glycosphingolipids, predominantly ceramide trihexoside.<sup>14</sup> As a direct result, lipid deposits can be

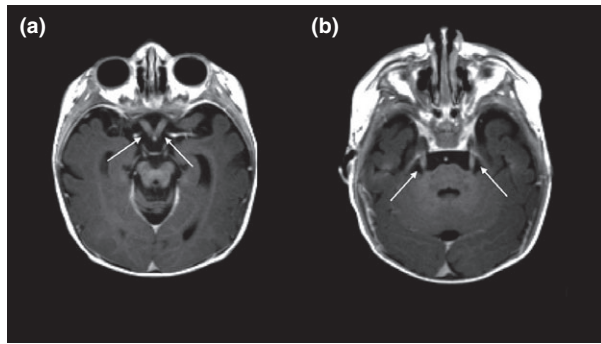


**Fig. 9.** While CN enhancement can be seen in many different forms of LSD, enlarged and enhancing optic nerves bilaterally (a, arrows) are typically seen in cases of Krabbe's disease. In this case, bilateral trigeminal nerve enhancement (b, arrows) is also present.



**Fig. 10.** Axial non-contrast-enhanced CT (NECT) image at the level of the thalami in a 4-year-old boy with Krabbe's disease. An imaging finding in Krabbe disease that only few LSD exhibit is increased attenuation within the bilateral thalami (arrows) early in the course of the disease on NECT. In addition, there is decreased bifrontal periventricular density (arrowheads) from demyelination.

seen within the ganglion cells of the dorsal root and autonomic nervous system, as well as specific cortical and brain stem structures.<sup>15</sup> Lipid deposits can be found in non-neural structures such as the cornea, glomeruli and tubules of the kidneys, cardiac myocytes and endothelial cells of blood vessels.<sup>15</sup> FD is an X-Linked disorder, however, a portion of females affected with the mutation may also develop disease-related complications with onset typically being delayed.<sup>16</sup> In late childhood or adolescence, affected patients begin to develop recurrent attacks of burning pain in their distal extremities. Angiokeratomas, or telangiectatic skin lesions, often occur over the area between the nipple line and above

the knees. Focal deficits, such as bilateral hearing loss, may develop.<sup>17</sup> Patients may also experience gastrointestinal symptoms, excessive sweating and vasomotor problems secondary to autonomic dysfunction.<sup>18</sup>

Endothelial blood vessel deposition of lipid leads to vascular events such as myocardial ischemia and dementia from multifocal strokes, most commonly in the early fourth through the sixth decade of life.<sup>19</sup> However, young men are at an increased risk for stroke as well, particularly in the vertebrobasilar system.<sup>20</sup> Thus, a common neuroimaging finding is multifocal infarcts within the small vessel distribution<sup>21</sup> (Fig. 11), tortuosity and dolichoectasia of cerebral vasculature particularly in the vertebrobasilar system which can lead to compressive or ischaemic dysfunction.

If imaging is performed on asymptomatic patients, non-specific, asymmetric, widespread deep white matter nodules that are hyperintense on T2 imaging may be seen (Fig. 11a). Increased T1 signal in the deep grey matter nuclei from remote ischaemic insult and mineralization, particularly in the lateral pulvinar, is considered pathognomonic (Fig. 11b).<sup>22</sup>

### Neuronal ceroid lipofuscinoses

Neuronal ceroid lipofuscinoses (NCL) is a heterogeneous group of lysosomal storage disorders that are generally classified as CLN1 to CLN10 and differ based on age of onset, clinical symptoms, neurophysiologic abnormalities and pathologic findings.<sup>23</sup> The pathophysiology is poorly understood and involves intracellular accumulation of an auto fluorescent lipopigment in neurons and other cells leading to progressive loss of nerve cells.<sup>24</sup> NCL demonstrates mostly an autosomal recessive pattern of inheritance.<sup>25</sup> Age of onset ranges from less than 2 years of age to adulthood with varying clinical presentations and life expectancies.<sup>1</sup> Patients who present before the age of 2 are said to have the infantile form and typically present with seizures and visual loss.

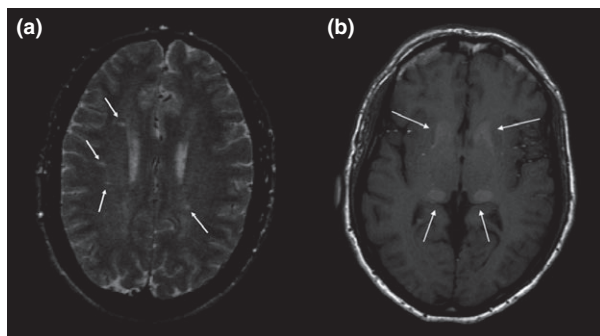


**Fig. 11.** Axial T2 (a) and T1 (b) image in a patient with Fabry disease. Image (a) demonstrates multiple foci of abnormal T2 hyperintensity within the white matter (arrows) representing multiple small infarcts. Image (b) shows increased T1 signal in bilateral basal ganglia and posterior thalami (arrows) representing mineralization secondary to remote infarctions.

The juvenile form is between 4 and 10 years of age with visual loss the most common presenting feature. Finally, patients present with adult disease around 30 years of age with seizures or abnormalities as the most common form of presentation.<sup>1</sup> All forms develop progressive ataxia, epilepsy and dementia.<sup>25</sup> The infantile and juvenile forms show progressive visual failure and retinopathy which is absent in late presentation cases (>30 years).<sup>26</sup> Patients with the disease demonstrate typical EEG abnormalities such as variable slowing of background activity, paroxysmal bursts of polyphasic epileptiform discharges and excessive photic response.<sup>25</sup>

On MRI, patients with NCL may demonstrate diffuse cerebral, as well as cerebellar atrophy.<sup>25</sup> Like the other lysosomal storage diseases, reduced T2/FLAIR signal is evident in the bilateral thalami.<sup>25</sup> This finding is most frequently associated with the infantile form followed by the juvenile.<sup>25</sup> Mild white matter and internal capsule T2 hyperintensity may also be seen, again, more commonly associated with the infantile form<sup>25</sup> (Fig. 12).

### Mucopolysaccharidoses

The mucopolysaccharidoses are another heterogeneous group of disorders resulting from various individual deficiencies of lysosomal enzymes that are involved in the degradation of glycosaminoglycans.<sup>27,28</sup> Manifestations of central nervous system involvement are related to excessive perivascular and intraneuronal storage of mucopolysaccharides.<sup>28</sup> Age of presentation and symptomatology are dependent on the particular disease. Hunter and Hurler usually present before the age of 10, while others may present in the teenage or young adult years.<sup>29, 30</sup> Symptoms at time of presentation vary by specific disease.

Magnetic resonance imaging findings vary in frequency and severity depending on the disease. Cerebral white matter lesions due to delayed myelination and/or demyelination secondary to accumulation of macromolecules seen as hyperintense T2 signal foci in periventricular white matter, dilated perivascular spaces including the basal ganglia, and meningeal thickening, are common.<sup>29,30</sup> Macrocrania early in the disease with associated hydrocephalus and arachnoid cyst formation is often seen in Hunter and Hurler's<sup>29,30</sup> (Fig. 13). Kyphoscoliosis, ligamentous thickening with atlantoaxial subluxation and cord compression can be seen and is a common cause of death in Morquio disease<sup>29,30</sup> (Fig. 14). Hepatosplenomegaly and cardiac dysfunction are accompanying manifestations of the disease outside the CNS.

### Gangliosidoses

Gangliosides are complex lipids that are predominately found in the brain grey matter. Disorders of ganglioside metabolism are identified on the basis of specific underlying enzyme deficiency and the resultant accumulation

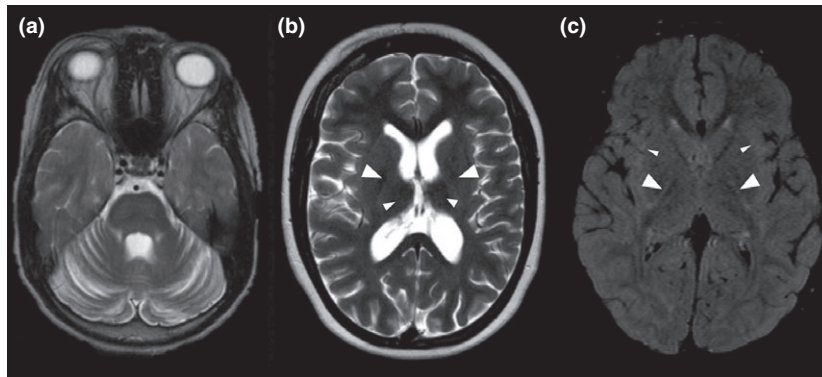


**Fig. 12.** Axial T2's (a and b) and axial FLAIR with fat saturation (c) images in patients with NCL at varying ages. Image (a) depicts cerebellar atrophy in a 9-year-old patient. Patients with the infantile and juvenile forms of the disease often have decreased T2 signal in the thalami (small arrowheads) and basal ganglia (large arrowheads) as evident in image (b) in a 12-year-old patient. Mild white matter (small arrowheads) and internal capsule (large arrowheads) T2/FLAIR hyperintensity in a 15-month-old as seen in image (c) is more commonly associated with the infantile form.

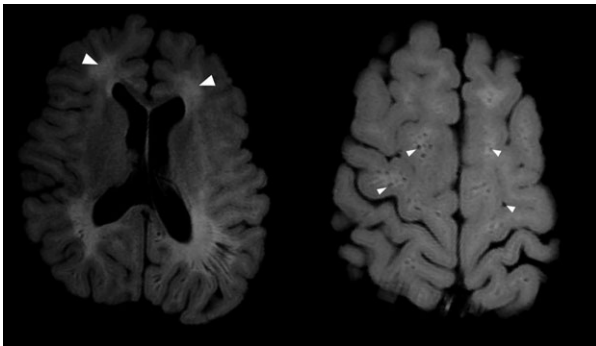


**Fig. 13.** Axial FLAIR T2 images with fat saturation in a 6-year-old patient with Hurler's syndrome showing hyperintense T2 signal foci in periventricular white matter (large arrowheads) and dilated perivascular spaces (short arrowheads).

of its substrate. Two common forms exist: GM1 gangliosidosis and GM2 gangliosidosis.

GM1 gangliosidosis is associated with the neuronal storage of the monosialoganglioside GM1. This ganglioside alone constitutes 20% of the gangliosides found in the brain and 80% found in myelin.<sup>1</sup> The disease is a direct result of a deficiency in the enzyme beta-galactosidase. This enzyme is responsible for the cleavage of the terminal galactose of GM1.<sup>1</sup> Deficiency of the enzyme is a result of one of 102 described genetic mutations.<sup>31</sup> Decreased enzymatic activity results in incomplete metabolism of several other substrates such as galactose containing glycoproteins, *N*-acetylgalactosamine, lactose and keratan sulfate.<sup>1</sup> Early infantile, infantile and juvenile forms are described. In early infantile, dysmorphic facial features, such as frontal bossing, gingival hypertrophy and thickened alveolar ridges may be present at birth.<sup>1</sup> Hepatosplenomegaly is usually appreciated within the first few months of life. The late infantile form has an onset between 12 and 18 months and usually manifest with gait disturbances and frequent falls.<sup>1</sup> Skeletal

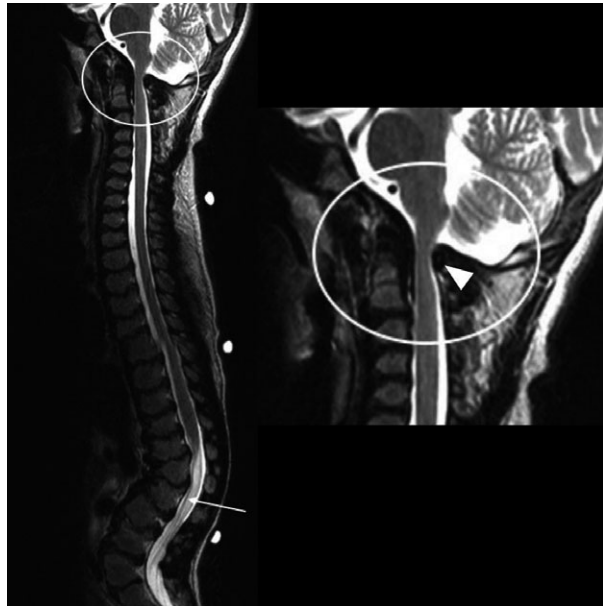


**Fig. 14.** Sagittal T2-weighted image of the spine in a patient with Morquio disease showing bullet-shaped vertebral bodies and thickened intervertebral discs characteristic of mucopolysaccharidoses. There is gibbus formation (arrow) centered at L1 with no significant mass effect on the cauda equina. At cervical level, the posterior arcus of the atlas is hypoplastic (arrowhead) predisposing to repetitive atlantoaxial subluxation and reactive ligamentous thickening at its posterior aspect resulting in significant cord compression near the foramen magnum (circle).

deformities such as hypoplasia of the acetabula and proximal deformity of the metacarpal bones may be evident in both early and late.<sup>1</sup> Patients eventually develop spasticity, tonic spasms and pyramidal signs.<sup>1</sup> In the juvenile form, disease symptoms usually develop in late childhood or adolescence. Patients demonstrate a protracted clinical course with dysarthria and extrapyramidal signs.<sup>1</sup>

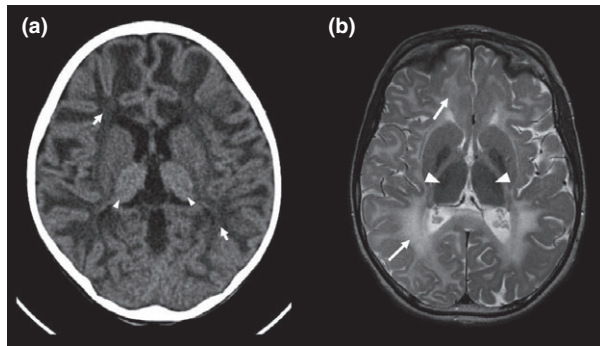


**Fig. 15.** (a) Axial NECT and (b) T2 weighted images through the thalami in 6-month-old patient with infantile GLD. Similar to many LSDs, the bilateral thalami demonstrate decreased signal on T2 (large arrowheads). However, a unique feature that is similar to Krabbe disease, is that the thalami are often hyperattenuating on NECT (small arrowheads). A way to separate the two is based on the patient's age. Because patients with infantile GLD tend to exhibit imaging findings earlier than Krabbe disease, the white matter is not fully mature with more fluid content. This is evident by the hypodense appearance of the white matter (short arrows) and increased T2 signal (long arrows) of the white matter when compared to the grey matter.

GM2 gangliosidosis has several variants, all of which are associated with the neuronal storage of the monosialoganglioside GM2. Primary accumulation of GM2 occurs secondary to mutations involving either the alpha or beta subunit of hexosaminidase A.<sup>32</sup> Mutation of the alpha subunit is classically referred to as Tay-Sachs disease with mutation of the beta as Sandhoff's. A variant exists where there is a mutation in the hexosaminidase-A protein, known as the AB variant.<sup>32</sup> Tay-Sachs is classically known to affect the Ashkenazi Jewish population. Similar to GM1 gangliosidosis, infantile and juvenile forms exist. Patients affected by Tay-Sachs disease have psychomotor deterioration and exaggerated startle response to loud noise.<sup>1</sup> Macrocephaly is most prominent in the second year of life.<sup>1</sup> Patients also exhibit axial hypotonia, bilateral pyramidal signs and blindness.<sup>1</sup> The hallmark of the disease, however, is the classic macular cherry-red spot. During the more terminal stages, patients develop generalized tonic-clonic and/or minor motor seizures.<sup>1</sup> Unlike GM1, patients who have Tay-

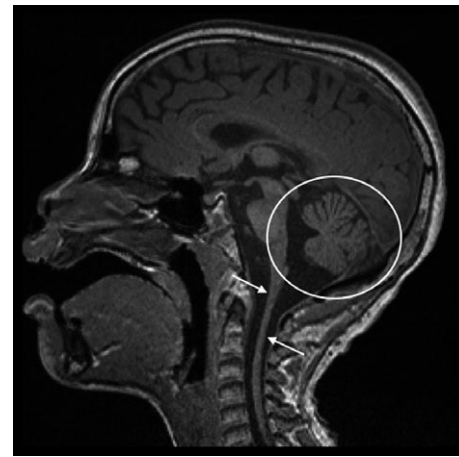


**Fig. 16.** The sagittal T1-weighted image in a patient with juvenile GLD shows cerebellar (circle) and spinal cord (arrows) atrophy. While cerebellar involvement can be seen in all variants, spinal cord atrophy is typically characteristic of the juvenile and adult forms.

Sachs do not exhibit dysmorphic facies, hepatosplenomegaly or skeletal deformities.<sup>1</sup> Later onset Tay-Sachs disease can manifest in either childhood, adolescents or adulthood. Patients will usually follow a more protracted course. There is no predilection to a certain ethnic group like for the infantile form.<sup>1</sup> Patients develop dysarthria and walking problems secondary to spastic paraparesis or proximal muscle weakness.<sup>1</sup> Cerebellar atrophy is prominent in the later-onset forms.<sup>1</sup> Like the infantile form, some patients will eventually begin to have tonic-clonic or myoclonic seizures.<sup>1</sup> Sandhoff's disease differs from Tay-Sachs in a few subtle ways. Patients afflicted by Sandhoff's usually have hepatosplenomegaly and N-acetylglucosamine-containing oligosaccharides in the urine.<sup>1</sup>

Neuroimaging characteristics are somewhat shared between the subtypes. In the infantile forms of both GM1 and GM2 gangliosidosis, gyral enlargement due to atrophy is common.<sup>33</sup> Mild cerebellar involvement may be present, however, usually corpus callosum is spared early in the disease process with thalamic and cerebellar atrophy being a sequela of late disease.<sup>33</sup> T2 hypointense signal is again seen within the bilateral thalami

**Table 1.** Summary of guidelines for MR imaging approach of LSDs

Tigroid white matter	Cerebellar atrophy	Macrocephaly	Cranial nerve enhancement	Early corpus callosum involvement	Spinal cord atrophy
<ul style="list-style-type: none"> <li>• Metachromatic Leukodystrophy</li> <li>• Krabbe's Disease</li> <li>• Gangliosidoses</li> <li>• Mucopolysaccharidoses</li> </ul>	<ul style="list-style-type: none"> <li>• Neuronal Ceroid Lipofuscinosis</li> <li>• Gangliosidoses</li> <li>• Metachromatic Leukodystroph y (Late)</li> </ul>	<ul style="list-style-type: none"> <li>• Gangliosidoses (GM1 or GM2)</li> <li>• Metachromatic Leukodystrophy (early)</li> <li>• Mucopolysaccharidoses (Hunter &amp; Hurler)</li> </ul>	<ul style="list-style-type: none"> <li>• Metachromatic Leukodystrophy</li> <li>• Krabbe's Disease</li> </ul>	<ul style="list-style-type: none"> <li>• Krabbe's Disease</li> </ul>	<ul style="list-style-type: none"> <li>• Gangliosidoses (Juvenile GM2)</li> </ul>

(Fig. 15). Symmetric diffuse, faintly tigroid appearance can also be seen within the cerebral white matter on T2-weighted imaging much like the other LSD.<sup>33</sup> The juvenile and adult forms of the gangliosidosis demonstrate spinal cord anterior horn atrophy which is often more extensive than the brain (Fig. 16). Patients with late onset Tay-Sachs may have areas of restricted diffusion in periventricular white on DWI.<sup>33</sup> Findings on MR spectroscopy are similar to MLD with a decrease in NAA and relative increase in choline and myo-inositol in the infantile form.<sup>33</sup> Juvenile disease may show decreased NAA in otherwise normal appearing thalami and white matter.<sup>33</sup>

In conclusion, while the LSDs have very discrete enzymatic causes, there is an overlap in symptomatology and CNS imaging findings. However, certain imaging features are more prevalent among certain disorders and can help narrow the differential diagnosis and sometimes point to the correct diagnosis. Table 1 is a summary of guidelines for MR imaging approach of LSDs.

## References

- Pastores G. Lysosomal storage diseases. In: Swaiman K, ed. *Swaiman's Pediatric Neurology: Principles and Practice*, 5th edn. Elsevier Health Sciences, New York, 2012: 403–51.
- der van Voom JP, Pouwels PJW, Kamphorst W *et al.* Histopathologic correlates of radial stripes on MR images in lysosomal storage disorders. *AJNR Am J Neuroradiol* 2005; **26**: 442–6.
- Gieselmann V. Metachromatic leukodystrophy: recent research developments. *J Child Neurol* 2003; **18**: 591.
- Gieselmann V, Franken S, Klein D *et al.* Metachromatic leukodystrophy: consequences of sulphatide accumulation. *Acta Paediatr Suppl* 2003; **92**: 74.
- Biffi A, Cesani M, Fumagalli F *et al.* Metachromatic leukodystrophy – mutation analysis provides further evidence of genotype-phenotype correlation. *Clin Genet* 2008; **74**: 349–57.
- Baumann N, Turpin JC, Lefevre M *et al.* Motor and psycho-cognitive clinical types in adult metachromatic leukodystrophy: Genotype/phenotype relationships? *J Physiol Paris* 2002; **96**: 301.
- Ito K, Miura N, Awata S *et al.* A case of adult onset metachromatic leukodystrophy. *Psychiatry Clin Neurosci* 2009; **63**: 127.
- Vettoretto N, Giovanetti M, Regina P *et al.* Hemorrhagic cholecystitis as a likely cause of nontraumatic hemobilia in metachromatic leukodystrophy: report of a case. *Ann Ital Chir* 2001; **72**: 725.
- Kim TS, Kim IO, Kim WS *et al.* MR of childhood metachromatic leukodystrophy. *AJNR Am J Neuroradiol* 1997; **18**: 773–738.
- Suzuki K. Globoid cell leukodystrophy (Krabbe's disease): update. *J Child Neurol* 2003; **18**: 595.
- Wenger DA, Rafi MA, Luzi P. Molecular genetics of Krabbe disease (globoid cell leukodystrophy): diagnostic and clinical implications. *Hum Mutat* 1997; **10**: 268–79.
- Barone R, Bruhl K, Stoeter P, Fiumara A, Pavone L, Beck M. Clinical and neuroradiological findings in classic infantile and late-onset globoid-cell leukodystrophy (Krabbe disease). *Am J Med Genet* 1996; **63**: 209–17.
- Randell E, Connolly-Wilson M, Duff A *et al.* Evaluation of the accuracy of enzymatically determined carrier status for Krabbe disease by DNA-based testing. *Clin Biochem* 2000; **33**: 217.
- de Veber GA, Schwarting GA, Kolodny EH, Kowall NW. Fabry disease: immunocytochemical characterization of neuronal involvement. *Ann Neurol* 1992; **31**: 409–15.
- MacDermot KD, Holmes A, Miners AH. Anderson-Fabry disease: Clinical manifestations and impact of disease in a cohort of 98 hemizygous males. *J Med Genet* 2001; **38**: 750.
- MacDermot KD, Holmes A, Miners AH. Anderson-Fabry disease: clinical manifestations and impact of disease in a cohort of 60 obligate carrier females. *J Med Genet* 2001; **38**: 769.
- Germain DP, Avan P, Chassaing A *et al.* Patients affected with Fabry disease have an increased incidence of progressive hearing loss and sudden deafness: an investigation of twenty-two hemizygous male patients. *BMC Med Genet* 2002; **3**: 10.
- Kolodny EH, Pastores GM. Anderson-Fabry disease: extrarenal, neurologic manifestations. *J Am Soc Nephrol* 2002; **13**: 150.
- Desnick RJ, Ioannou YA, Eng CM. Alpha-galactosidase A deficiency: Fabry disease. In: Scriver CR, Beaudet AL, Sly WS, Valle D (eds). *The Metabolic and Molecular Bases of Inherited Disease*, 8th edn. McGraw-Hill, New York, 2001; 3733–74.
- Mitsias P, Levine SR. Cerebrovascular complications of Fabry's disease. *Ann Neurol* 1996; **40**: 8–17.
- Lidove O, Klein I, Lelievre J *et al.* Imaging features of Fabry disease. *AJR* 2006; **186**: 1184–91.
- Takanashi J, Barkovich AJ, Dillon WP, Sherr EH, Hart KA, Packman S. T1 hyperintensity in the pulvinar: key imaging feature for diagnosis of Fabry disease. *AJNR Am J Neuroradiol* 2003; **24**: 916–21.
- Muzaffar NE, Pearce DA. Analysis of NCL proteins from an evolutionary standpoint. *Curr Genom* 2008; **9**: 115–36.
- Goebel HH, Sharp JD. The neuronal ceroid-lipofuscinoses, recent advances. *Brain Pathol* 1998; **8**: 151–62.
- Rakesh H, Jadav MD. Clinical, electrophysiological, imaging, and ultrastructural description in 68 patients with neuronal ceroid lipofuscinoses and its subtypes. *Ped Neurol* 2014; **50**: 85–95.
- Vadlamudi L, Westmoreland BF, Klass DW, Parisi JE. Electroencephalographic findings in Kufs disease. *Clin Neurophysiol* 2003; **114**: 1738–43.

27. Clarke L. The mucopolysaccharidoses: a success of molecular medicine. *Expert Rev Mol Med* 2008; **10**: e1. doi: 10.1017/S1462399408000550
28. Zoltan P. Diffusion-weighted MR imaging in leukodystrophies. *Eur Radiol* 2005; **15**: 2284–303.
29. Kendall BE. Lysosomes, peroxisomes, and mitochondria: function and disorder. *AJNR Am J Neuroradiol* 1992; **13**: 621–54.
30. der van Knaap M, Valk J. Magnetic Resonance of Myelination and Myelin Disorders, 3rd edn. Springer, Berlin, 2005.
31. Brunetti-Pierri N, Scaglia F. GM1 gangliosidosis: review of clinical, molecular, and therapeutic aspects. *Mol Genet Metab* 2008; **94**: 391.
32. Fernandes Filho JA, Shapiro BE. Tay-Sachs disease. *Arch Neurol* 2004; **61**: 1466.
33. Chen C, Zimmerman R, Lee C, Chen F, Yuh Y, Hsiao H. Neuroimaging findings in late infantile GM1 gangliosidosis. *AJNR Am J Neuroradiol* 1998; **19**: 1628–30.